






ORIGINAL RESEARCH

Association of Region-Specific Cardiac Adiposity With Dysglycemia and New-Onset Diabetes

Kuo-Tzu Sung , MD; Jen-Yuan Kuo, MD; Chun-Ho Yun, MD, PhD; Yueh-Hung Lin, MD; Jui-Peng Tsai, MD, PhD; Chi-In Lo, MD; Chih-Chung Hsiao, MD; Yau-Huei Lai, MD; Cheng-Ting Tsai , MD; Charles Jia-Yin Hou , MD; Cheng-Huang Su, MD, PhD; Hung-I Yeh , MD, PhD; Chen-Yen Chien, MD, PhD; Ta-Chuan Hung, MD; Chung-Lieh Hung , MD, MPH, PhD

BACKGROUND: Visceral adipose tissue is assumed to be an important indicator for insulin resistance and diabetes beyond overweight/obesity. We hypothesized that region-specific visceral adipose tissue may regulate differential biological effects for new-onset diabetes regardless of overall obesity.

METHODS AND RESULTS: We quantified various visceral adipose tissue measures, including epicardial adipose tissue, paracardial adipose tissue, interatrial fat, periaortic fat, and thoracic aortic adipose tissue in 1039 consecutive asymptomatic participants who underwent multidetector computed tomography. We explored the associations of visceral adipose tissue with baseline dysglycemic indices and new-onset diabetes. Epicardial adipose tissue, paracardial adipose tissue, interatrial fat, periaortic fat, and thoracic aortic adipose tissue were differentially and independently associated with dysglycemic indices (fasting glucose, postprandial glucose, HbA1c, and homeostasis model assessment of insulin resistance) beyond anthropometric measures. The superimposition of interatrial fat and thoracic aortic adipose tissue on age, sex, body mass index, and baseline homeostasis model assessment of insulin resistance expanded the likelihood of baseline diabetes (from 67.2 to 86.0 and 64.4 to 70.8, P for $\Delta \chi^2$: <0.001 and 0.011 , respectively). Compared with the first tertile, the highest interatrial fat tertile showed a nearly doubled risk for new-onset diabetes (hazard ratio, 2.09 [95% CI, 1.38–3.15], $P<0.001$) after adjusting for Chinese Visceral Adiposity Index.

CONCLUSIONS: Region-specific visceral adiposity may not perform equally in discriminating baseline dysglycemia or diabetes, and showed differential predictive performance in new-onset diabetes. Our data suggested that interatrial fat may serve as a potential marker for new-onset diabetes.

Key Words: diabetes ■ epicardial adipose tissue ■ interatrial fat ■ periaortic fat ■ thoracic aortic adipose tissue ■ visceral adipose tissue

The global obesity epidemic is jeopardizing public health, and its prevalence has increased nearly 3-fold over the past 4 decades, as reported by the World Health Organization.¹ Obesity, as excessive whole-body adiposity, contributes to the development of numerous cardiovascular diseases (CVD), including hypertension, metabolic abnormality, and coronary artery disease.^{2–4} Among obesity-related metabolic

disorders, insulin resistance and type 2 diabetes are major contributors to excessive risk of CVD and all-cause mortality.^{5–7} Obesity per se is associated with risk of diabetes, and local and ectopic adiposity possibly play a central pathophysiological role in mediating insulin resistance and glucose intolerance. Greater amounts of abdominal visceral adipose tissue (VAT), rather than subcutaneous fat, are more closely

Correspondence to: Chung-Lieh Hung, MD, MSc, PhD, Division of Cardiology, Department of Internal Medicine, Mackay Memorial Hospital, Zhongshan North Rd, 10449, Taipei, Taiwan. E-mail: jotaro3791@gmail.com

Supplemental Material for this article is available at <https://www.ahajournals.org/doi/suppl/10.1161/JAHA.121.021921>

For Sources of Funding and Disclosures, see page 11.

© 2021 The Authors. Published on behalf of the American Heart Association, Inc., by Wiley. This is an open access article under the terms of the Creative Commons Attribution-NonCommercial-NoDerivs License, which permits use and distribution in any medium, provided the original work is properly cited, the use is non-commercial and no modifications or adaptations are made.

JAHA is available at: www.ahajournals.org/journal/jaha

CLINICAL PERSPECTIVE

What Is New?

- Various visceral adiposity measures showed differential correlations with dysglycemic indices including insulin resistance.
- Interatrial fat may serve as a useful new surrogate for subjects at higher risk of new-onset diabetes.

What Are the Clinical Implications?

- Utilization of region-specific visceral adiposity independently correlated with dysglycemic indices beyond anthropometric measures.
- Interatrial fat and thoracic aortic adipose tissue improved risk stratification in identifying new-onset diabetes.

Nonstandard Abbreviations and Acronyms

EAT	epicardial adipose tissue
IAF	interatrial fat
PARF	periaortic fat
PAT	paracardial adipose tissue
TAT	thoracic aortic adipose tissue
VAT	visceral adipose tissue

associated with insulin resistance and higher levels of circulating adipocytokines and subsequent adverse systemic metabolic effects.^{8,9}

With advances in several imaging modalities, including computed tomography (CT) or magnetic resonance imaging, a vast amount of literature has emerged on the heightened metabolic and CVD risks of region-specific excessive visceral fat (eg, pericardial, abdominal, and periaortic fat).^{10–14} Epidemiological studies and meta-analyses have demonstrated a link between larger visceral adiposity depots and diabetes risk,¹⁵ although data on the differential impacts of region-specific visceral adiposity on the incidence of new-onset diabetes are scarce. Because type 2 diabetes has been proposed as a coronary heart disease equivalent,¹⁶ diabetic risk prediction using a data set originally designed for coronary atherosclerotic burden likely provides additional clinical values on integrated CVD risk assessment.

This study aims to investigate the potential differential utilization of region-specific visceral adiposity surrounding the heart in predicting incident diabetes. We further examine whether visceral adiposity may provide incremental values beyond conventional anthropometrics in new-onset diabetes.

METHODS

Because of the sensitive nature of the data collected for this study, requests to access the data set from qualified researchers trained in human subject confidentiality protocols may be sent to “MacKay Memorial Hospital” Institutional Data Access/Ethics Committee for researchers (Institutional Review Board contact information: MacKay Memorial Hospital. Address: No. 92, Sec. 2, Zhongshan N. Rd, Taipei City 10449, Taiwan. TEL: 02-25433535#3486–3488, E-mail: mmhirb82@gmail.com).

Study Subjects

This prospective study enrolled asymptomatic individuals who underwent a cardiovascular health survey (June 2009 to December 2012) at MacKay Memorial Hospital, a tertiary referral medical center in Northern Taiwan. All study participants underwent comprehensive history taking, physical examination, anthropometric measures (including body mass index [BMI], waist circumference, and body fat composition), and blood sampling tests. Thoracic multidetector computed tomography (MDCT) scanning for the coronary calcification burden (as coronary calcium score) was performed in all participants for cardiovascular risk stratification. We defined the overweight/obese and lean groups by BMI cutoffs of ≥ 23 and < 23 kg/m², respectively.¹⁷ Hypertension was defined as a systolic and/or diastolic blood pressure ≥ 140 and ≥ 90 mm Hg, respectively, or antihypertensive medication use, and the diagnosis was confirmed with a repeat test. Diabetes was diagnosed from fasting or postprandial glucose ≥ 126 or ≥ 200 mg/dL, respectively, or a HbA1c $\geq 6.5\%$ on 2 occasions, known history of clinically diagnosed diabetes, or active treatment with antidiabetic medication. Prediabetes was defined as the absence of prior diabetes history with fasting or postprandial glucose > 99 or > 140 mg/dL, respectively, or HbA1c $> 5.6\%$. The normoglycemic group included participants without a history of diabetes, fasting or postprandial glucose ≤ 99 or ≤ 140 mg/dL, respectively, and HbA1c $\leq 5.6\%$. New-onset diabetes was defined as a postenrollment new diagnosis of diabetes based on the American Diabetes Association criteria¹⁸ in nondiabetic participants using the MDCT study day as index date. The primary outcome of this study was the event of new-onset diabetes. The follow-up period ended when the study participants developed new-onset diabetes before May 4, 2017, and censored events were scored for those who died before or lived beyond May 4, 2017 without a new-onset diabetes. The study setting is published elsewhere.¹⁹ Because of retrospective study design, informed consent was waived for study

participants. The study protocol complied with the Declaration of Helsinki and was approved by the institutional review board of MacKay Memorial Hospital with IRB number: 14MMHIS202.

Body Fat Composition, Adiposity, and Biomarkers Analysis

Body fat composition was assessed by bioelectrical impedance analysis from foot-to-foot impedance estimate using the Tanita-305 Body-Fat Analyzer (Tanita Corp, Tokyo, Japan). The Chinese Visceral Adiposity Index (CAVI) was defined as $-267.93+0.68\times\text{Age}+0.03\times\text{BMI}+4.00\times\text{WC}+22.00\times\text{Log}_{10}\text{TG}-16.32\times\text{HDL-C}$ in male and $-187.32+1.71\times\text{Age}+4.23\times\text{BMI}+1.12\times\text{WC}+39.76\times\text{Log}_{10}\text{TG}-11.66\times\text{HDL-C}$ (TG: triglyceride, HDL-C: high-density lipoprotein, WC, waist circumference).²⁰ A Body Shape Index (ABSI) was calculated using the Krakauer and Krakauer equation based on an allometric regression: $\text{ABSI}=\text{WC}/(\text{BMI}^{2/3}\times\text{height}^{1/2})$.²¹ The index of homeostasis model assessment of insulin resistance (HOMA-IR) was available in 522 subjects and was calculated as: $\text{HOMA-IR}=\text{fasting insulin concentration (mU/mL)}\times\text{fasting glucose (mg/dL)}/22.5$. High-sensitivity C-reactive protein was quantified by a highly sensitive, latex particle-enhanced immunoassay (Elecsys 2010; Roche Diagnostics GmbH, Mannheim, Germany).

MDCT-Determined Visceral Adiposity Assessment

By using the MDCT data set for coronary calcium score, the VAT burden, based on 3D-volumetric quantification of epicardial adipose tissue (EAT; adipose tissue volume [mL] located within the pericardial sac), periaortic fat (PARF), and thoracic aortic adipose tissue (TAT), was quantified using a dedicated workstation (Aquarius 3D Workstation; TeraRecon, San Mateo, CA, USA).^{19,22,23} Paracardial adipose tissue (PAT) was defined as the adipose tissue surrounding the heart outside the parietal pericardium. We calculated the average of maximum of both axial diameters and their perpendicular diameters of paracardial fat at right costophrenic angle (Figure 1).²⁴ For volume measures of EAT, PAT, TAT, and PARF, visceral fat tissue was defined as pixels within a window from -195 to -45 HU and a window center at -120 HU. The TAT was defined as the whole adipose tissue volume (mL) surrounding the thoracic aorta, involving an area 67.5 mm caudal to the bifurcation level of the pulmonary arteries. PARF borders were manually traced over the pericardium in axial images from 8 slices that extended cranially 24 mm from the level of the left main coronary artery; thus, all adipose volume (mL) surrounding the aortic root within the pericardial sac but over the EAT was selected as PARF. Cross-sectional fatty areas were

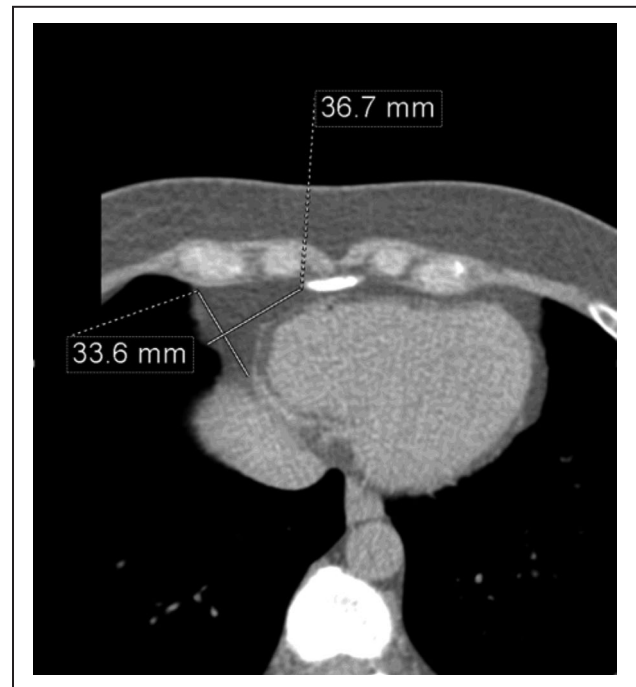


Figure 1. Measurement of PAT at the right costophrenic angle in MDCT.

The PAT was measured by utilizing the most optimal axial computed tomography image of PAT and calculated the average value of the maximum of axial diameter and the perpendicular diameter of PAT at the right costophrenic angle. MDCT indicates multidetector computed tomography; and PAT, paracardial adipose tissue.

quantified by summing the pixels within different axial images and multiplying them by the slice thickness to obtain fat volumes. For interatrial fat (IAF), the imaging plane was further adjusted into a horizontal long-axis view for the IAF assessment defined as the adipose tissue thickness located between the left and right atria, which was measured by acquiring IAF thickness on horizontal and long-axis planes.^{22,23,25,26} Imaging acquisition protocol along with more detailed IAF measure by MDCT is further detailed in Figure S1.

Statistical Analysis

Data are expressed as mean \pm SDs and percentage (%) for continuous and categorical variables, respectively. The clinical characteristics and the quantification of EAT, PAT, IAF, PARF, and TAT were compared across normoglycemic, prediabetic, and diabetic groups using 1-way ANOVA for normally distributed continuous or χ^2 test for categorical variables. Multiple pairwise comparisons for continuous variables among the groups were made by post hoc tests (Bonferroni correction) after ANOVA.

The diagnostic/discriminative performance for prevalent type 2 diabetes by region-specific VAT and optimal cutoffs chosen (as maximal Youden Index)

was assessed using receiver operating characteristic curves. Univariate and multivariate linear regression was used to assess the significance of cross-sectional associations in the regional fat between the pericardial/myocardial/periaortic fat and diabetes-related parameters, including fasting glucose, postprandial glucose, HbA1c, and HOMA-IR, and high-sensitivity C-reactive protein. Each model was adjusted for age, sex, BMI/WC/body fat composition, estimated glomerular filtration rate, total cholesterol, and HDL levels.

Multivariate Cox regression models were used to examine the associations of region-specific VAT with new-onset diabetes. Individual hazard ratio (HR) and correspondent 95% CI were obtained. Key clinical covariates including age, sex, anthropometric indices, medical histories, and dysglycemic indices served as confounders. Using a time-dependent receiver-operator characteristic analysis (Harrell's C-statistics) by Cox regression model, we further additionally analyzed the predictive value of the various VAT in predicting new-onset type 2 diabetes; DeLong's test was used to compare the differences between the 2 AUCs from the different models. Kaplan–Meier failure analysis and the log-rank test for *P*-trend across tertiles of EAT, PAT, IAF, PARF, and TAT were performed for determining the incidence of new-onset diabetes.

Analyses were performed in STATA 14.2, StataCorp. A 2-tailed probability value <0.05 was considered statistically significant.

RESULTS

Study Subjects

Among 1039 participants (mean age 50.9±9.1 years; 261 [25.1%] women and 778 [74.9%] men), the mean EAT, PAT, IAF, PARF, and TAT volumes were 74.8±27.9 cm³, 22.8±8.2 mm, 8.56±0.83 mm, 21.0±10.2 cm³, and 7.1±3.6 cm³, respectively. Baseline characteristics and regional fat depots across normoglycemic, prediabetic, and diabetic groups were compared (Table 1). Participants with prediabetes and diabetes tended to be older, have higher BMI, have higher systolic and diastolic blood pressures, worse dysglycemic indices (fasting glucose, postprandial glucose, and HbA1c, higher HOMA-IR), and unfavorable lipid profiles (higher serum triglyceride level, lower HDL-C level), higher serum high-sensitivity C-reactive protein level, and coronary calcium burden (all trend *P*<0.01). A graded and remarkably greater PAT, IAF, and TAT rather than EAT or PARF were observed across nondiabetic, prediabetic, and diabetic groups, respectively (all trend *P*<0.001), indicating that excessive PAT, IAF, and TAT depots may be observed in earlier stages along the dysglycemic spectrum (Table 1; all trend *P*<0.05). EAT, PARF, and TAT were all larger in

overweight/obese versus lean subjects regardless of diabetes status except for IAF (*P*=0.54).

We illustrated that the IAF volume is greater in obese than in lean participants in the nondiabetic group (Figure 2C), but without significant differences of IAF volume between obese and lean participants with diabetes. This manifestation is quite different from EAT, PAT, PARF, and TAT, wherein fat volume was significantly greater in obese participants with diabetes than in their lean counterparts (Figure 2A, 2B, 2D, 2E). Obese participants had greater accumulation of EAT, PARF, and TAT than lean participants, but there was no interaction effect for body size and amounts of cardiovascular fat depots in 4 different regions.

C-statistics of EAT, PAT, IAF, PARF, and TAT were 0.64, 0.60, 0.68, 0.67, and 0.68 with cutoff values of 79.5 cm³, 36 mm, 8.5 mm, 18.1 cm³, and 7.2 cm³, respectively (Table 2). In the univariate model, EAT, PAT, PARF, IAF, and TAT were all significantly associated with fasting glucose, postprandial glucose, HOMA-IR, HbA1c, and high-sensitivity C-reactive protein (all *P*<0.05) (Table S1). All visceral adiposity measures were significantly associated with neutrophil-to-lymphocyte ratio in univariate model (all *P*<0.05) except for EAT, which showed borderline significance (*P*=0.065). After adjusting for age, sex, lipid profiles, and anthropometric measures, the EAT, PARF, and TAT remained significantly associated with insulin resistance (HOMA-IR; all *P*<0.05), with both IAF and TAT independently associated with fasting or postprandial glucose, and HbA1c (all *P*<0.01). Furthermore, PAT, IAF, and TAT were independently associated with neutrophil-to-lymphocyte ratio (all *P*<0.05). IAF and TAT, rather than EAT or PARF, remarkably expanded the likelihood ratio of identifying baseline diabetes (χ^2 : from 67.2 to 86.0 and 64.4 to 70.8, *P* for ΔW^2 : <0.001 and 0.011, respectively) when superimposed on age, sex, BMI, and baseline HOMA-IR. Details are addressed in Data S1.

EAT, PAT, IAF, PARF, and TAT were all positively correlated with BMI/WC. Differential correlations were observed among various visceral adiposity, BMI, body fat composition, and WC. (Table S2). Additionally, all visceral adiposity measures were positively associated with coronary calcification burden, with PAT demonstrating lowest correlation (Table S3).

Region-Specific Visceral Fat and New-Onset Diabetes

During a median 3.72-year (interquartile range: 1.57–7.4 years) follow-up duration, there were 187 subjects with new-onset diabetes among 913 participants without baseline diabetes. By Cox proportional regression model, IAF and TAT were closely associated with new-onset diabetes even after multivariate adjustment. IAF for those who remained in normoglycemic condition at

Table 1. Baseline Characteristics and the Volume of Various Visceral Adiposity Measures in Normoglycemic, Prediabetic, and Diabetic Groups

	All participants (n=1039)	Normoglycemic group (n=324)	Prediabetic group (n=589)	Diabetic group (n=126)	(ANOVA) P Value
Demographic data					
Age, y	50.9±9.1	48.7±8.8	51.1±8.8*	55.2±9.3*†	<0.001
Female, number (%)	261 (25.1)	105 (32.4)	130 (22.1)	26 (20.6)	0.001
SBP, mm Hg	122.6±17.0	118.3±15.4	123.2±16.6*	130.7±19.4*†	<0.001
DBP, mm Hg	76.0±10.7	74.8±10.4	76.0±10.8	79.3±10.9*†	<0.001
Pulse pressure, mm Hg	46.5±12.1	43.5±10.1	47.2±12.1*	51.4±14.4*†	<0.001
Heart rate, bpm	66.5±11.2	65.7±11.7	66.7±11.1	67.8±10.4	0.31
Hypertension, number (%)	187 (18.0)	44 (13.6)	91 (15.5)	52 (42.3)	<0.001
Cardiovascular disease, number (%)	64 (6.1)	14 (4.3)	29 (4.9)	21 (16.7)	<0.001
Hyperlipidemia, number (%)	79 (7.6)	23 (7.1)	37 (6.3)	19 (15.1)	0.04
Smoking, number (%)	160 (15.4)	60 (18.5)	76 (12.9)	24 (19.1)	0.45
Regular exercise, number (%)	185 (17.8)	65 (20.1)	95 (16.1)	25 (19.8)	0.54
Biochemical data					
Fasting glucose, mg/dL	102.2±24.9	90.8±5.7	99.4±8.8*	144.9±50.1*†	<0.001
Postprandial glucose, mg/dL	121.9±49.9	105.8±24.4	113.3±30.2	196.4±82.9*†	<0.001
HbA1c, mg/dL	5.9±0.9	5.4±0.3	5.8±0.3*	7.5±1.5*†	<0.001
HOMA-IR	1.9±1.7	1.4±0.9	1.8±1.5*	3.1±2.9*†	<0.001
Total cholesterol, mg/dL	200.0±34.9	196.1±33.5	203.0±34.9*	196.4±37.2	0.007
Triglyceride, mg/dL	137.0±89.3	114.9±65.9	140.7±85.5*	177.6±133.2*†	<0.001
LDL, mg/dL	129.7±31.3	126.4±28.9	132.4±31.8*	125.6±33.8	0.008
HDL, mg/dL	51.9±13.5	55.2±14.6	51.3±12.6*	46.7±12.5*†	<0.001
Neutrophil-to-lymphocyte ratio	1.90±0.88	1.79±0.95	1.91±0.81	2.13±0.96*†	<0.001
hs-CRP, mg/L	0.16±0.24	0.16±0.25	0.16±0.23	0.23±0.26*†	0.007
eGFR, mL/min per 1.73 m ²	86.4±15.6	87.8±15.6	85.4±14.8	86.8±18.8	0.08
Measurement of body adiposity					
Body mass index, kg/m ²	24.3±3.2	23.7±2.8	24.4±3.2*	25.5±3.4*†	<0.001
Waist circumference, cm	83.6±9.0	81.1±8.6	83.9±8.6*	88.8±8.9*†	<0.001
Body fat composition, %	25.4±6.3	25.3±5.9	25.2±6.4	26.5±6.8	0.10
Body shape index	0.77±0.04	0.76±0.04	0.77±0.04	0.80±0.04	<0.001
Chinese Visceral Adiposity Index	88.1±37.8	75.7±34.6	89.3±36.4	115.1±37.5	<0.001
MDCT-determined visceral adiposity					
EAT, cm ³	74.8±27.9	71.3±28.6	74.5±27.1	85.4±27.3*†	<0.001
PAT, mm	22.8±8.2	21.7±8.5	22.8±7.8*	25.8±9.1*†	<0.001
IAF, mm	8.56±0.83	8.36±0.76	8.55±0.80*	9.08±0.92*†	<0.001
PARF, cm ³	21.0±10.2	19.3±9.8	20.7±9.8	26.6±10.9*†	<0.001
TAT, cm ³	7.1±3.6	6.3±3.5	7.1±3.3*	9.3±4.2*†	<0.001
MDCT-derived coronary calcium score					
Coronary calcium score	37.4±146.8	21.7±90.9	41.0±168.8*	60.9±148.6*†	<0.001

bpm indicates beats per minute; DBP, diastolic blood pressure; EAT, epicardial adipose tissue; eGFR, estimated glomerular filtration rate; HDL, high-density lipoprotein; HOMA-IR, homeostasis model assessment of insulin resistance; hs-CRP, high-sensitivity C-reactive protein; IAF, interatrial fat; LDL, low-density lipoprotein; MDCT, multidetector computed tomography; PARF, periaortic fat; PAT, paracardial adipose tissue; SBP, systolic blood pressure; and TAT, thoracic aortic adipose tissue.

**P*<0.05 versus normoglycemic group.

†*P*<0.05 versus prediabetic group by pairwise comparisons using post hoc analysis.

follow-up without baseline prediabetes or diabetes was significantly lower (*n*=276, 7.68±0.35 cm³) compared with those who had either baseline diabetes or new-onset

diabetes at follow-up (*n*=313, 9.00±0.91 cm³). Per 1-SD increment of IAF, EAT, PAT, PARF, and TAT was associated with 1.7%, 1.3%, 1.4%, 1.4%, and 1.4% increase

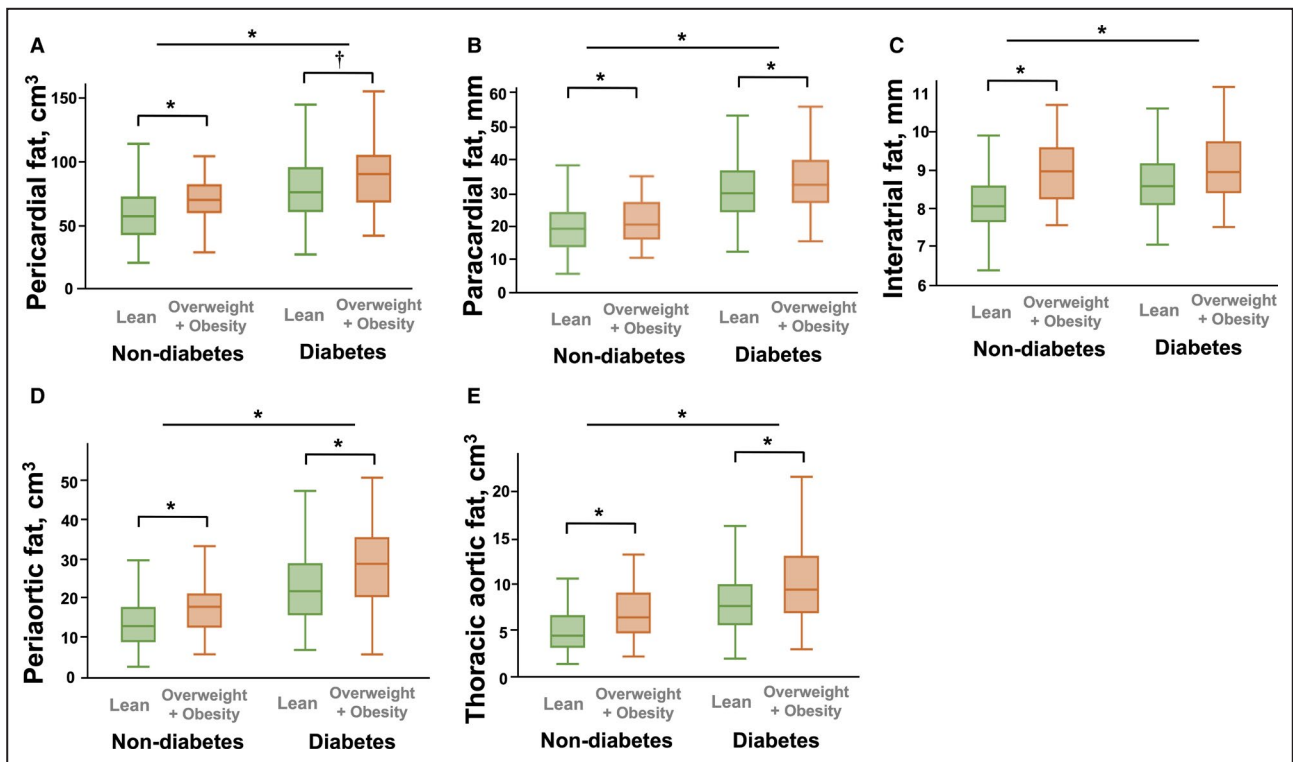


Figure 2. Volume of interatrial and periaortic fat in lean and obese groups across participants with diabetes and those without diabetes.

Comparison of different regions of fat volume in lean and obese groups across participants with diabetes and those without diabetes. **A**, Epicardial adipose tissue (EAT). **B**, Paracardial adipose tissue. **C**, Interatrial fat. **D**, Periaortic fat. **E**, thoracic aortic adipose tissue (TAT). Overweight/obese participants showed significantly larger region-specific visceral adipose tissue than lean participants without diabetes. The same differences were observed in participants with diabetes, except for interatrial fat. * $P < 0.001$, † $P < 0.05$. P value for difference between two cohorts based on ANOVA test.

in new-onset diabetes during follow-up, respectively (all $P < 0.001$), with a graded and significant increase of new-onset diabetes in larger region-specific VAT tertile groups (3rd versus 1st tertile, HR, 2.7, 1.8, 2.8, 2.7, and

2.2 [95% CI, 1.8–4.0, 1.3–2.6, 1.9–4.1, 1.8–4.0, and 1.4–3.2 for EAT, PAT, IAF, PARF, TAT, respectively], all log-rank $P < 0.05$; Figure 3A through 3E). However, greater tertile groups of PAT did not show increased risk of

Table 2. AUROC Curve, CI, Cut-off Point, Sensitivity, Specificity, Positive Predictive Value, and Negative Predictive Values of Anthropometrics and Various Visceral Adiposity Measures in Discriminating Prevalent Diabetes

Indicators of various adiposity	AUROC (95% CI)	Cut-off	Sensitivity, %	Specificity, %	PPV, %	NPV, %
Diabetes (dependent variable)						
Body mass index, kg/m ²	0.62 (0.57–0.68)	24.5	60.3	58.5	20.5	93.6
Waist circumference, cm	0.68 (0.63–0.73)	88.0	50.8	74.7	21.7	91.7
Body fat composition, %	0.56 (0.51–0.62)	33.6	14.0	90.5	17.3	88.1
A Body Shape Index	0.55 (0.51–0.60)	0.8	47.6	76.5	21.8	17.1
Chinese Visceral Adiposity Index	0.67 (0.62–0.71)	106.1	61.3	72.7	23.5	93.2
EAT, cm ³	0.64 (0.58–0.69)	79.5	59.3	65.0	18.5	92.3
PAT, mm	0.57 (0.52–0.63)	36.0	31.8	80.1	18.0	89.5
IAF, mm	0.68 (0.63–0.73)	8.5	70.4	55.0	17.8	93.1
PARF, cm ³	0.67 (0.62–0.72)	18.1	78.6	48.3	17.3	94.2
TAT, cm ³	0.68 (0.63–0.73)	7.2	64.4	59.7	17.6	92.6

Data from all adiposity indicators were standardized in models. AUROC indicates area under the receiver operating characteristic; EAT, epicardial adipose tissue; IAF, interatrial fat; NPV, negative predictive value; PARF, periaortic fat; PAT, paracardial adipose tissue; PPV, positive predictive value; and TAT, thoracic aortic adipose tissue.

new-onset diabetes after adjustment (3rd versus 1st tertile, log-rank $P > 0.05$).

A greater amount of EAT, IAF, and PARF demonstrated a higher risk of incident new-onset diabetes (3rd versus 1st tertile, HR, 1.7, 1.9, and 1.7 [95% CI, 1.1–2.7, 1.2–2.8, and 1.0–2.7, respectively], all $P < 0.05$) even after adjusting for CVAI (Table 3). Because CVAI alone showed modest predictive values of new-onset diabetes (Harrell's C-statistics: 0.67 [95% CI, 0.62–0.71]), addition of IAF on CVAI significantly expanded Harrell's C-statistics from 0.67 to 0.71 (P for Δ AUROC=0.03) in predicting new-onset diabetes. However, the addition of CVAI to EAT, PARF, and TAT showed no such incremental values in model prediction (Table 3) (Figure 4A through 4E).

DISCUSSION

Our findings are 3-fold: First, individuals with diabetes consistently had greater VAT burden than nondiabetics, with all VAT tightly associated with dysglycemic indices to various extents. In subjects with diabetes, those classified into overweight/obese showed larger VAT than those classified into the lean group except for IAF.

Secondly, IAF and TAT showed comparable discriminative ability in identifying baseline diabetes, with both superimposed on baseline clinical covariates substantially improving diagnostic performance. Thirdly, larger IAF not only showed independent associations with new-onset diabetes in fully adjusted models, but also provided incremental values in predicting new-onset diabetes during follow-up.

Association of Region-Specific Visceral Fat With Dysglycemia and Metabolic Derangements

Our current findings are consistent with previous reports wherein participants with diabetes and prediabetes have generally higher epicardial and periaortic fat burden,²⁷ with a strong and positive association between excessive visceral fat depots and several dysglycemic indices.^{15,28} Because ectopic fat deposits surrounding visceral organs (eg, heart or coronary artery vasculature) have been shown to be biologically active rather than passive fat stores, and have unique functional and anatomical characteristics,^{29,30} adipopathy ("sick fat") develops when adipose tissues

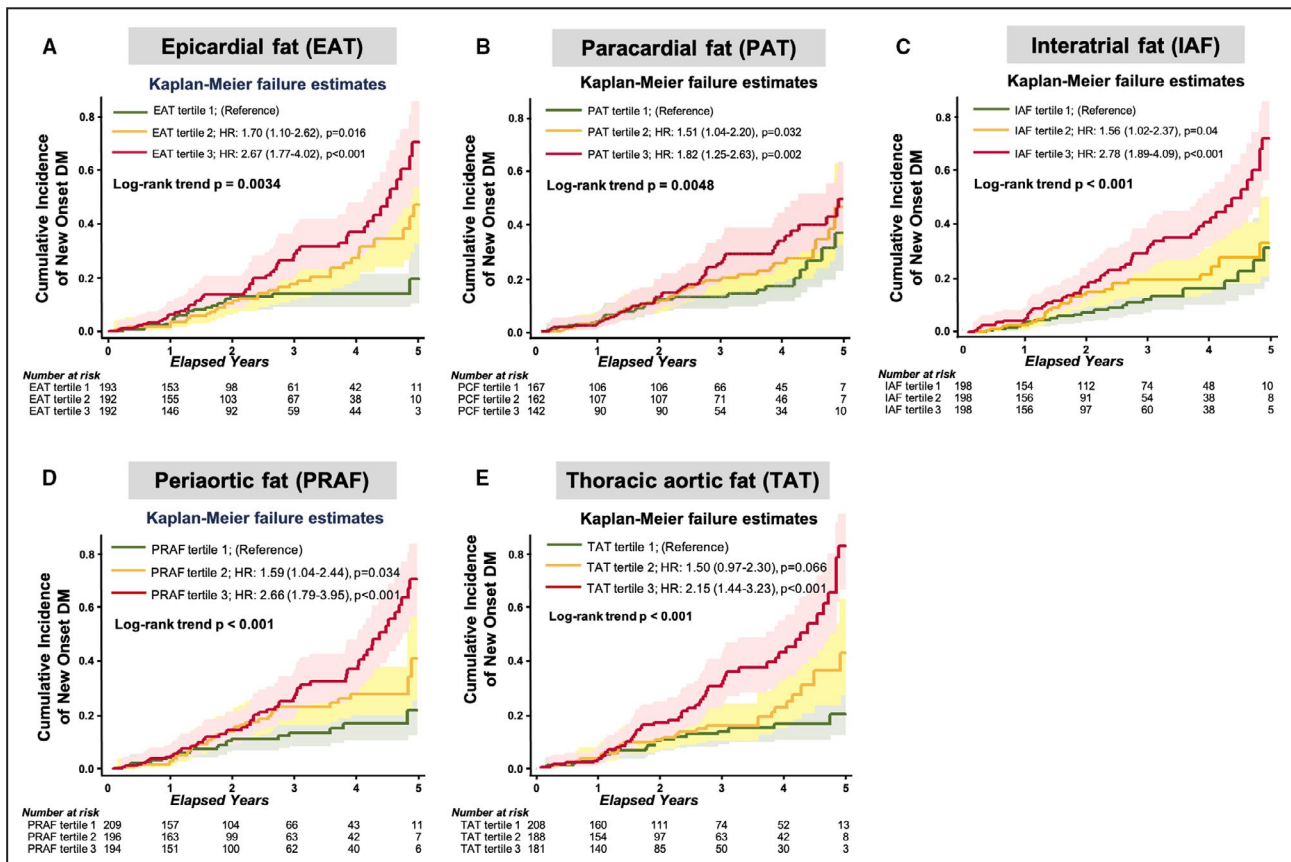


Figure 3. Kaplan-Meier curves for new-onset diabetes by various region-specific VAT.

There is a graded increase in the incidence of new-onset diabetes across tertiles of epicardial adipose tissue (A), paracardial adipose tissue (B), interatrial fat (C), periaortic fat (D), and thoracic aortic adipose tissue (E), with all log-rank trend $P < 0.05$. HR indicates hazard ratio; and VAT, visceral adipose tissue.

Table 3. Unadjusted and Adjusted Hazard Ratio for Various Visceral Adiposity Measures in Predicting New-Onset Diabetes

Types of visceral adiposity measures		Unadjusted			Adjusted for age + sex + BMI		Adjusted for age + sex + BMI + HOMA-IR		Adjusted for CVAI	
Event rate	Harrell C-statistic	Hazard ratio (95% CI)	P Value	Hazard ratio (95% CI)	P Value	Hazard ratio (95% CI)	P Value	Hazard ratio	P Value	
EAT	0.64 (0.60–0.69)									
Tertile 1	...	(reference)	...	(reference)	...	(reference)	...	(reference)	...	
Tertile 2	...	1.69 (1.10–2.62)	0.016	1.41 (0.90–2.19)	0.133	1.56 (0.84–2.89)	0.160	1.47 (0.93–2.31)	0.101	
Tertile 3	...	2.67 (1.77–4.01)	<0.001	1.73 (1.09–2.73)	0.019	1.60 (0.84–3.03)	0.150	1.88 (1.18–2.99)	0.008	
PAT	0.61 (0.56–0.65)									
Tertile 1	...	(reference)	...	(reference)	...	(reference)	...	(reference)	...	
Tertile 2	...	1.51 (1.03–2.20)	0.032	1.26 (0.86–1.84)	0.244	1.18 (0.72–1.92)	0.517	1.22 (0.83–1.80)	0.318	
Tertile 3	...	1.82 (1.25–2.63)	0.002	1.30 (0.88–1.93)	0.187	1.07 (0.63–1.84)	0.796	1.28 (0.86–1.90)	0.223	
TAT	0.65 (0.60–0.69)									
Tertile 1	...	(reference)	...	(reference)	...	(reference)	...	(reference)	...	
Tertile 2	...	1.50 (0.97–2.30)	0.060	1.12 (0.69–1.81)	0.333	1.00 (0.55–1.81)	0.989	1.06 (0.67–1.68)	0.792	
Tertile 3	...	2.15 (1.44–3.23)	<0.001	1.33 (0.78–2.25)	0.298	0.73 (0.37–1.44)	0.361	1.29 (0.67–1.68)	0.269	
PARF	0.66 (0.62–0.71)									
Tertile 1	...	(reference)	...	(reference)	...	(reference)	...	(reference)	...	
Tertile 2	...	1.59 (1.04–2.44)	0.034	1.25 (0.79–1.99)	0.338	1.07 (0.58–1.99)	0.831	1.23 (0.77–1.95)	0.389	
Tertile 3	...	2.66 (1.79–3.95)	<0.001	1.69 (1.04–2.73)	0.034	1.53 (0.79–2.94)	0.205	1.79 (1.12–2.85)	0.015	
IAF	0.67 (0.62–0.72)									
Tertile 1	...	(reference)	...	(reference)	...	(reference)	...	(reference)	...	
Tertile 2	...	1.56 (1.02–2.37)	0.040	1.34 (0.87–2.06)	0.181	1.39 (0.77–2.51)	0.273	1.37 (0.89–2.11)	0.148	
Tertile 3	...	2.78 (1.89–4.09)	<0.001	1.85 (1.21–2.83)	0.005	2.19 (1.25–3.84)	0.006	2.09 (1.38–3.15)	<0.001	

BMI indicates body mass index; CVAI, Chinese Visceral Adiposity Index; EAT, epicardial adipose tissue; HOMA-IR, homeostasis model assessment of insulin resistance; IAF, interatrial fat; PARF, periaortic fat; PAT, paracardial adipose tissue; and TAT, thoracic aortic adipose tissue.

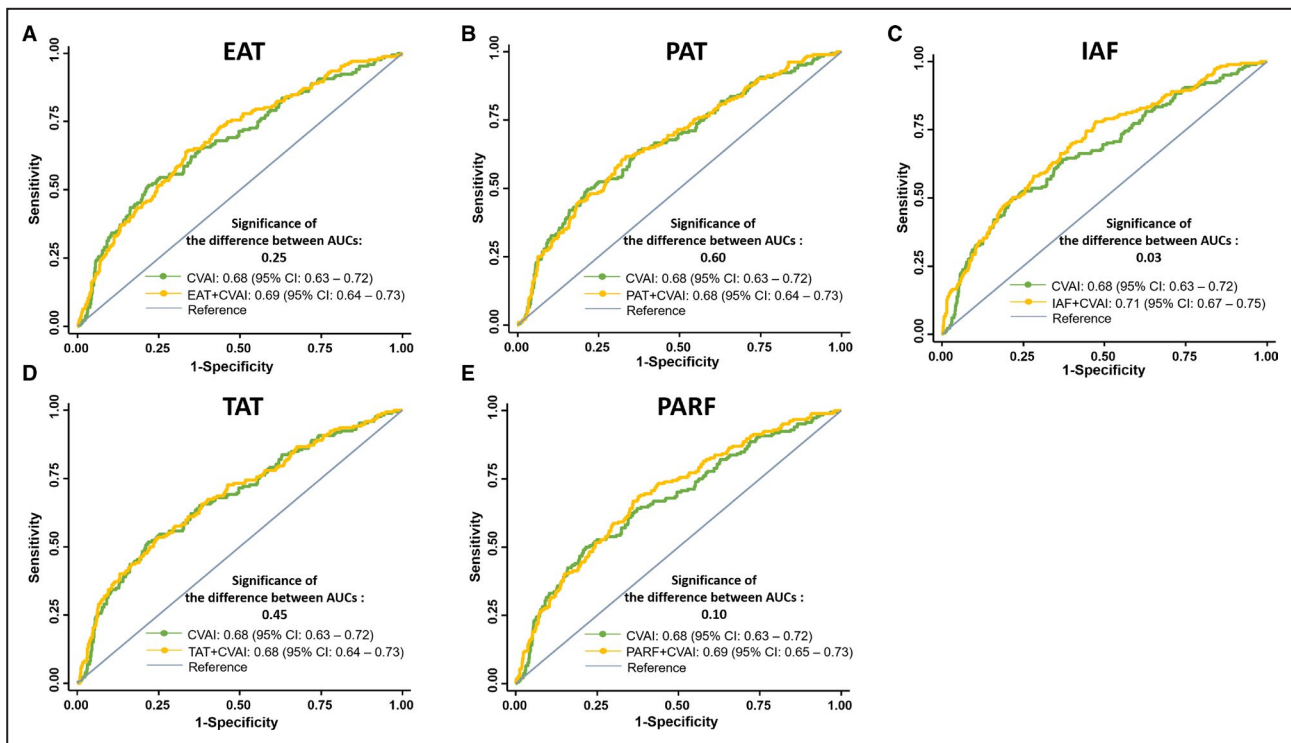


Figure 4. Harrell C-statistics of new-onset diabetes by adding various region-specific VAT to CVAI.

The area under the curve of new-onset diabetes by adding region-specific VAT on CVAI. **A**, Pericardial fat (EAT). **B**, Paracardial fat (PAT). **C**, Interatrial fat (IAF). **D**, Periaortic fat (PARF). **E**, Thoracic aortic adipose tissue (TAT). The addition of IAF to Chinese Visceral Adiposity Index (CVAI) demonstrated significant incremental values of the receiver operating characteristics curve in predicting new-onset diabetes by expanding Harrell's C-statistics from 0.68 to 0.71 (P value=0.03). VAT indicates visceral adipose tissue.

cause functional abnormalities through endocrinological, metabolic, and immunological derangements.³¹ Presence of visceral adiposopathy (sick fat) likely contributes to several metabolic disorders through secretion of bioactive adipokines and a variety of pro-inflammatory cytokines (eg, interleukin-1- β [IL-1- β], IL-6, tumor necrosis factor- α , resistin, omentin, and leptin) resulting in lipotoxicity in obese or dysglycemic individuals that may worsen cardiac function through paracrine and mechanical restriction.^{29–33}

Differential Biological or Pathological Correlates of Region-Specific Visceral Fat

In the current study, we observed the potentiality of differential associations of a variety of region-specific visceral fat with dysglycemia; while IAF, PAT, and TAT are more closely associated with glucose intolerance, EAT, PARF, and TAT appeared to be more tightly linked to insulin resistance. TAT surrounding the thoracic aorta as the closest fat depot to the pancreas can more directly secrete proinflammatory cytokines into the systemic circulation and may exert greater paracrine and vasoactive effects than fat depots surrounding or within the myocardium.^{25,34} Instead, PARF and TAT are perivascular fat deposits surrounding the proximal ascending and thoracic aorta and therefore may be closely

related to vasculopathy and the systemic inflammatory process.^{35,36} On the other hand, EAT is beige fat tissue whereas thoracic fat is brown fat tissue and may contain more mitochondria, and therefore these 2 may not have the same pro-inflammatory or vasoactive properties.³⁶ EAT is anatomically confined in the pericardial sac distant from the systemic circulation when compared with TAT or PAT and likely exerts a mechanical impact on the heart and coronary vasculopathy.^{30,37}

Interatrial Fat as a Novel Marker for New-Onset Diabetes

In the present study, the IAF volume remained significantly associated with the incidence of new-onset diabetes independent of BMI and insulin resistance (HOMA-IR). We demonstrated that IAF can be a novel surrogate marker for new-onset diabetes in an asymptomatic population with relatively low prevalent CVD (6.1%) that underwent cardiovascular health survey and risk stratification using MDCT-derived coronary calcium scoring.³⁸ Early recognition of higher diabetes risk in such a population likely facilitates more early therapeutic interventions for CVD from a primary preventive viewpoint, including lifestyle modification and pharmacological treatment.

Abnormal lipid storage in the cardiomyocytes is an early manifestation in diabetes pathogenesis; in this

Inter-atrial Fat (IAF)	Peri-vascular Fat (PARF or TAT)	Epicardial Adipose Tissue (EAT)	Paracardial Adipose Tissue (PAT)
Location Fat within inter-atrial area	Location Fat surrounding ascending aorta (PARF) and thoracic aorta (TAT)	Location Fat confined in epicardial sac ²⁴	Location Mediastinal fat outside the parietal pericardium surrounding the heart ²⁴
Biological effects Atrial electromechanical disturbances ²² Part of peri-atrial fat ²⁶ Oxidative phosphorylation activity Genetic profiles mimicking myocardium as marker of "Cardiac Steatosis" ^{39,40,44}	Biological effects Carotid arterial vasculopathy or atherosclerosis ²³ Circulating pro-inflammatory marker ^{25,34-36} Circulating cardiometabolic risk ²⁵	Biological effects Coronary vasculopathy or atherosclerosis ^{25,29} Mechanical Effect impeding cardiac diastolic function ^{29,30} Circulating pro-inflammatory marker ²⁵	Biological effects Menopause-specific effects on coronary artery atherosclerosis ²⁷
Clinical correlates <ul style="list-style-type: none"> Larger inter-atrial fat is associated with higher risk of HF hospitalization in HFpEF²² Increased inter-atrial fat correlated with higher incidence of new-onset diabetes 	Clinical correlates <ul style="list-style-type: none"> Increased thoracic aortic fat and peri-aortic fat are associated with aortic atherosclerosis or calcification^{36,41} Larger peri-aortic fat as part of visceral adiposity is associated with insulin resistance³⁴ 	Clinical correlates <ul style="list-style-type: none"> Larger epicardial fat as part of visceral adiposity is associated with insulin resistance/fasting glucose²⁷⁻²⁹ Implicated in HFpEF with obesity³⁰ 	Clinical correlates <ul style="list-style-type: none"> Pericardial fat is positively correlated with systemic metabolic parameters²⁴ Larger paracardial fat correlated with abdominal visceral fat²⁴

Figure 5. The mechanism of various visceral adiposity measures in different regions mediating insulin resistance, glucose intolerance, and cardiovascular risk. HFpEF indicates heart failure with preserved ejection fraction; and PARF, periaortic fat.

regard, myocardial lipid overaccumulation likely serves a marker of myocardial adiposity that causes myocardial lipotoxicity or "cardiac steatosis."^{22,39,40} As part of peri-atrial fat, IAF has been shown to be an atypical adipose tissue and behave biologically distinct from perivascular adiposity measures or epicardial fat, which are pathologically linked to the effect of systemic pro-inflammatory cytokines or directly involved in coronary vasculopathy.^{11,14,23,25,26,41} In our previous work, IAF has also been shown to affect atrial electromechanical properties in HFpEF.²² The unique genetic expressions of peri-atrial fat relating to oxidative phosphorylation and cardiac myocytes (eg, myofiber heavy chains and Ca²⁺ handling) likely imply that IAF may be metabolically active and tightly implicated in energy (glucose or free fatty acid) homeostasis with a strong interaction with myocardium.⁴² Compared with other adiposity measures, IAF was less associated with insulin resistance yet demonstrated strongest correlation with postprandial glucose in the present study (Table S1). These findings from IAF also replicated features of cardiac steatosis, which has been shown to be an earlier manifestation of glucose intolerance (postprandial glucose level) preceding the onset of diabetes and that insulin resistance was not an independent determinant driving myocardial steatosis.^{43,44} Taken collectively, we speculated that peri-atrial fat may be more susceptible to early metabolic derangement (eg, diabetes) and perhaps may share similar biological features of myocardial adiposity as a marker of cardiac steatosis. Nevertheless, further mechanistic studies will be required to clarify these issues. The location, assumed biological effect, and clinical correlation of EAT, PAT, IAF, PARF, and TAT in mediating insulin resistance and glucose intolerance are further summarized in Figure 5.

Limitations

Firstly, our current study was retrospective in study design and was limited to data from a single center; therefore, our findings may not apply to other populations in the same way. Secondly, a causal relationship and precise mechanistic link between interatrial adiposity and dysglycemia or incident diabetes could not be established, partly because of a relative lack of published literature data on IAF genomic and proteomic expression features. Future studies to address these relevant issues may be warranted to solve this issue. Thirdly, our current data set did not allow accurate measures of abdominal fat, intermuscular fat, and hepatic fat content, and therefore comparisons of region-specific adiposity measures relating to diabetes were only available for fat surrounding the heart and aorta.

CONCLUSIONS

In a large-scale asymptomatic Asian population, region-specific visceral adiposity may manifest differential biological effects. Interatrial fat likely represents part of myocardial adiposity, which may serve as a new surrogate marker for new onset of diabetes. Our findings emphasize the clinical implications for utilizing region-specific visceral fats in identifying high-risk individuals prone to the development of adiposopathy-related dysglycemia or diabetes.

ARTICLE INFORMATION

Received April 3, 2021; accepted November 9, 2021.

Affiliations

Division of Cardiology, Department of Internal Medicine, MacKay Memorial Hospital, Taipei, Taiwan (R.O.C.) (K.S., J.K., C.Y., Y.L., J.T., C.L., C.H., Y.L., C.T., C.J.H., C.S., H.Y., T.H., C.H.); Department of Medicine, MacKay Medical

College, New Taipei City, Taiwan (R.O.C.) (K.S., J.K., Y.L., J.T., C.L., C.H., C.T., C.J.H., C.S., H.Y., C.C., T.H., C.H.); MacKay Medicine, Nursing, and Management College, Taipei, Taiwan (R.O.C.) (J.K., C.Y., Y.L., C.T., C.J.H., C.S., H.Y., C.C., T.H.); Division of Radiology (C.Y.), and Cardiovascular Division, Department of Surgery (C.C.), MacKay Memorial Hospital, Taipei, Taiwan (R.O.C.); Institute of Clinical Medicine, National Yang Ming Chao Tung University, Taipei, Taiwan (R.O.C.) (K.S., Y.L.); Division of Cardiology, Department of Internal Medicine, MacKay Memorial Hospital, Hsinchu, Taiwan (R.O.C.) (Y.L.); and Institute of Biomedical Sciences, MacKay Medical College, New Taipei City, Taiwan (R.O.C.) (C.H.).

Sources of Funding

This research was supported by the Ministry of Science and Technology (Taiwan) (grants NSC-101-2314-B-195-020, NSC103-2314-B-010-005-MY3, 103-2314-B-195-001-MY3, 101-2314-B-195-020-MY1, MOST 103-2314-B-195-006-MY3, and NSC102-2314-B-002-046-MY3, 106-2314-B-195-008-MY2, 108-2314-B-195-018-MY2, 109-2314-B-715-008, 110-2314-B-715-009-MY1), MacKay Memorial Hospital (10271, 10248, 10220, 10253, 10375, 10358, E-102003), and the Taiwan Foundation for geriatric emergency and critical care.

Disclosures

All the authors have nothing to disclose.

Supplemental Material

Data S1

Tables S1–S3

Figures S1

REFERENCES

- Fernberg U, op 't Roodt J, Fernström M, Hurtig-Wennlöf A. Body composition is a strong predictor of local carotid stiffness in Swedish, young adults – the cross sectional Lifestyle, biomarkers, and atherosclerosis study. *BMC Cardiovasc Disord*. 2019;19:205. doi: 10.1186/s12872-019-1180-6
- Bell JA, Carslake D, O'Keefe LM, Frysz M, Howe LD, Hamer M, Wade KH, Timpson NJ, Smith GD. Associations of body mass and fat indexes with cardiometabolic traits. *J Am Coll Cardiol*. 2018;72:3142–3154. doi: 10.1016/j.jacc.2018.09.066
- Kachur S, Lavie CJ, de Schutter A, Milani RV, Ventura HO. Obesity and cardiovascular diseases. *Minerva Med*. 2017;108:212–228. doi: 10.23736/S0026-4806.17.05022-4
- Lavie CJ, Milani RV, Ventura HO. Obesity and cardiovascular disease: risk factor, paradox, and impact of weight loss. *J Am Coll Cardiol*. 2009;53:1925–1932. doi: 10.1016/j.jacc.2008.12.068
- Xu L, Chan WM, Hui YF, Lam TH. Association between HbA1c and cardiovascular disease mortality in older Hong Kong Chinese with diabetes. *Diabet Med*. 2012;29:393–398. doi: 10.1111/j.1464-5491.2011.03456.x
- Cavero-Redondo I, Peleteiro B, Álvarez-Bueno C, Rodríguez-Artalejo F, Martínez-Vizcaino V. Glycated haemoglobin A1c as a risk factor of cardiovascular outcomes and all-cause mortality in diabetic and non-diabetic populations: a systematic review and meta-analysis. *BMJ Open*. 2017;7:e015949. doi: 10.1136/bmjopen-2017-015949
- Zhang X, Li J, Zheng S, Luo Q, Zhou C, Wang C. Fasting insulin, insulin resistance, and risk of cardiovascular or all-cause mortality in non-diabetic adults: a meta-analysis. *Biosci Rep*. 2017;37. doi: 10.1042/BSR20170947
- Hayashi T, Boyko EJ, Leonetti DL, McNeely MJ, Newell-Morris L, Kahn SE, Fujimoto WY. Visceral adiposity and the risk of impaired glucose tolerance: a prospective study among Japanese Americans. *Diabetes Care*. 2003;26:650–655. doi: 10.2337/diacare.26.3.650
- Indulekha K, Anjana RM, Surendar J, Mohan V. Association of visceral and subcutaneous fat with glucose intolerance, insulin resistance, adipocytokines and inflammatory markers in Asian Indians (CURES-113). *Clin Biochem*. 2011;44:281–287. doi: 10.1016/j.clinbiochem.2010.12.015
- Wong CX, Ganesan AN, Selvanayagam JB. Epicardial fat and atrial fibrillation: current evidence, potential mechanisms, clinical implications, and future directions. *Eur Heart J*. 2017;38:1294–1302. doi: 10.1093/eurheartj/ehw045
- Cavalcante JL, Tamarappoo BK, Hachamovitch R, Kwon DH, Alraies MC, Halliburton S, Schoenhagen P, Dey D, Berman DS, Marwick TH. Association of epicardial fat, hypertension, subclinical coronary artery disease, and metabolic syndrome with left ventricular diastolic dysfunction. *Am J Cardiol*. 2012;110:1793–1798. doi: 10.1016/j.amjcard.2012.07.045
- Iacobellis G, Ribaudo MC, Assael F, Vecci E, Tiberti C, Zappaterreno A, Mario UD, Leonetti F. Echocardiographic epicardial adipose tissue is related to anthropometric and clinical parameters of metabolic syndrome: a new indicator of cardiovascular risk. *J Clin Endocrinol Metab*. 2003;88:5163–5168. doi: 10.1210/jc.2003-030698
- Thanassoulis G, Massaro JM, O'Donnell CJ, Hoffmann U, Levy D, Ellinor PT, Wang TJ, Schnabel RB, Vasani RS, Fox CS, et al. Pericardial fat is associated with prevalent atrial fibrillation: the Framingham Heart Study. *Circ Arrhythm Electrophysiol*. 2010;3:345–350. doi: 10.1161/CIRCEP.109.912055
- Brinkley TE, Leng X, Chughtai HL, Nicklas BJ, Kritchevsky SB, Ding J, Kitzman DW, Hundley WG. Periaortic fat and cardiovascular risk: a comparison of high-risk older adults and age-matched healthy controls. *Int J Obes (Lond)*. 2014;38:1397–1402. doi: 10.1038/ijo.2014.29
- Li Y, Liu B, Li Y, Jing X, Den S, Yan Y, She Q. Epicardial fat tissue in patients with diabetes mellitus: a systematic review and meta-analysis. *Cardiovasc Diabetol*. 2019;18:3. doi: 10.1186/s12933-019-0807-3
- Juutilainen A, Lehto S, Rönönen T, Pyörälä K, Laakso M. Type 2 diabetes as a "coronary heart disease equivalent": an 18-year prospective population-based study in Finnish subjects. *Diabetes Care*. 2005;28:2901–2907. doi: 10.2337/diacare.28.12.2901
- Consultation WHOE. Appropriate body-mass index for Asian populations and its implications for policy and intervention strategies. *Lancet*. 2004;363:157–163.
- Members of the ADA Professional Practice Committee. Classification and diagnosis of diabetes: standards of medical care in diabetes-2020. *Diabetes Care*. 2020;43:S14–S31. doi: 10.2337/dc20-S002
- Huang BH, Chang SC, Yun CH, Sung K-T, Lai Y-H, Lo C-I, Huang W-H, Chien S-C, Liu LY-M, Hung T-C, et al. Associations of region-specific visceral adiposity with subclinical atrial dysfunction and outcomes of heart failure. *ESC Heart Fail*. 2020;7:3545–3560. doi: 10.1002/ehf2.12761
- Xia M-F, Chen Y, Lin H-D, Ma H, Li X-M, Aleteng Q, Li Q, Wang D, Hu YU, Pan B-S, et al. A indicator of visceral adipose dysfunction to evaluate metabolic health in adult Chinese. *Sci Rep*. 2016;6:38214. doi: 10.1038/srep38214
- Bawadi H, Abouwatfa M, Alsaed S, Kerkadi A, Shi Z. Body shape index is a stronger predictor of diabetes. *Nutrients*. 2019;11:1018. doi: 10.3390/nu11051018
- Hung C-L, Yun C-H, Lai Y-H, Sung K-T, Bezerra HG, Kuo J-Y, Hou C-Y, Chao T-F, Bulwer BE, Yeh H-I, et al. An observational study of the association among interatrial adiposity by computed tomography measure, insulin resistance, and left atrial electromechanical disturbances in heart failure. *Medicine (Baltimore)*. 2016;95:e3912. doi: 10.1097/MD.0000000000003912
- Yun C-H, Longenecker CT, Chang H-R, Mok GSP, Sun J-Y, Liu C-C, Kuo J-Y, Hung C-L, Wu T-H, Yeh H-I, et al. The association among peri-aortic root adipose tissue, metabolic derangements and burden of atherosclerosis in asymptomatic population. *J Cardiovasc Comput Tomogr*. 2016;10:44–51. doi: 10.1016/j.jcct.2015.10.002
- Lim C, Ahn MI, Jung JI, Beck KS. Simple quantification of paracardial and epicardial fat dimensions at low-dose chest CT: correlation with metabolic risk factors and usefulness in predicting metabolic syndrome. *Jpn J Radiol*. 2018;36:528–536. doi: 10.1007/s11604-018-0752-1
- Yun C-H, Lin T-Y, Wu Y-J, Liu C-C, Kuo J-Y, Yeh H-I, Yang F-S, Chen S-C, Hou C-Y, Bezerra HG, et al. Pericardial and thoracic peri-aortic adipose tissues contribute to systemic inflammation and calcified coronary atherosclerosis independent of body fat composition, anthropometric measures and traditional cardiovascular risks. *Eur J Radiol*. 2012;81:749–756. doi: 10.1016/j.ejrad.2011.01.035
- Shin SY, Yong HS, Lim HE, Na JO, Choi CU, Choi JI, Kim SH, Kim JW, Kim EJ, Park SW, et al. Total and interatrial epicardial adipose tissues are independently associated with left atrial remodeling in patients with atrial fibrillation. *J Cardiovasc Electrophysiol*. 2011;6:647–655. doi: 10.1111/j.1540-8167.2010.01993.x
- Yang FS, Yun CH, Wu TH, Hsieh YC, Bezerra HG, Liu CC, Wu YJ, Kuo JY, Hung CL, Hou CY, et al. High pericardial and peri-aortic adipose tissue burden in pre-diabetic and diabetic subjects. *BMC Cardiovasc Disord*. 2013;13:98. doi: 10.1186/1471-2261-13-98

28. Iacobellis G, Barbaro G, Gerstein HC. Relationship of epicardial fat thickness and fasting glucose. *Int J Cardiol*. 2008;128:424–426. doi: 10.1016/j.ijcard.2007.12.072
29. González N, Moreno-Villegas Z, González-Bris A, Egido J, Lorenzo Ó. Regulation of visceral and epicardial adipose tissue for preventing cardiovascular injuries associated to obesity and diabetes. *Cardiovasc Diabetol*. 2017;16:44. doi: 10.1186/s12933-017-0528-4
30. Obokata M, Reddy YNV, Pislaru SV, Melenovsky V, Borlaug BA. Evidence supporting the existence of a distinct obese phenotype of heart failure with preserved ejection fraction. *Circulation*. 2017;136:6–19. doi: 10.1161/CIRCULATIONAHA.116.026807
31. Bays HE. Adiposopathy is "sick fat" a cardiovascular disease? *J Am Coll Cardiol*. 2011;57:2461–2473. doi: 10.1016/j.jacc.2011.02.038
32. Mazurek T, Zhang L, Zalewski A, Mannion JD, Diehl JT, Arafat H, Sarov-Blat L, O'Brien S, Keiper EA, Johnson AG, et al. Human epicardial adipose tissue is a source of inflammatory mediators. *Circulation*. 2003;108:2460–2466. doi: 10.1161/01.CIR.0000099542.57313.C5
33. Konishi M, Sugiyama S, Sato Y, Oshima S, Sugamura K, Nozaki T, Ohba K, Matsubara J, Sumida H, Nagayoshi Y, et al. Pericardial fat inflammation correlates with coronary artery disease. *Atherosclerosis*. 2010;213:649–655. doi: 10.1016/j.atherosclerosis.2010.10.007
34. Yudkin JS, Eringa E, Stehouwer CD. "Vasocrine" signalling from perivascular fat: a mechanism linking insulin resistance to vascular disease. *Lancet*. 2005;365:1817–1820. doi: 10.1016/S0140-6736(05)66585-3
35. Mancio J, Oikonomou EK, Antoniadou C. Perivascular adipose tissue and coronary atherosclerosis. *Heart*. 2018;104:1654–1662. doi: 10.1136/heartjnl-2017-312324
36. Chatterjee TK, Stoll LL, Denning GM, Harrelson A, Blomkalns AL, Idelman G, Rothenberg FG, Neltner B, Romig-Martin SA, Dickson EW, et al. Proinflammatory phenotype of perivascular adipocytes: influence of high-fat feeding. *Circ Res*. 2009;104:541–549. doi: 10.1161/CIRCRESAHA.108.182998
37. El Khoudary SR, Shields KJ, Janssen I, Budoff MJ, Everson-Rose SA, Powell LH, Matthews KA. Postmenopausal women with greater pericardial fat have more coronary artery calcification than premenopausal women: the Study of Women's Health Across the Nation (SWAN) cardiovascular fat ancillary study. *J Am Heart Assoc*. 2017;6:e004545. doi: 10.1161/JAHA.116.004545
38. Greenland P, Blaha MJ, Budoff MJ, Erbel R, Karol EW. Coronary calcium score and cardiovascular risk. *J Am Coll Cardiol*. 2018;72:434–447. doi: 10.1016/j.jacc.2018.05.027
39. Sharma S, Adrogue JV, Golfman L, Uray I, Lemm J, Youker K, Noon GP, Frazier OH, Taegtmeier H. Intramyocardial lipid accumulation in the failing human heart resembles the lipotoxic rat heart. *FASEB J*. 2004;18:1692–1700. doi: 10.1096/fj.04-2263com
40. Izzo P. Myocardial, perivascular, and epicardial fat. *Diabetes Care*. 2011;34:S371–S379. doi: 10.2337/dc11-s250
41. Lehman SJ, Massaro JM, Schlett CL, O'Donnell CJ, Hoffmann U, Fox CS. Peri-aortic fat, cardiovascular disease risk factors, and aortic calcification: the Framingham Heart Study. *Atherosclerosis*. 2010;210:656–661. doi: 10.1016/j.atherosclerosis.2010.01.007
42. Gaborit B, Venticlef N, Ancel P, Pelloux V, Gariboldi V, Leprince P, Amour J, Hatem SN, Jouve E, Dutour A, et al. Human epicardial adipose tissue has a specific transcriptomic signature depending on its anatomical peri-atrial, peri-ventricular, or peri-coronary location. *Cardiovasc Res*. 2015;108:62–73. doi: 10.1093/cvr/cvv208
43. McGavock JM, Lingvay I, Zib I, Tillery T, Salas N, Unger R, Levine BD, Raskin P, Victor RG, Szczepaniak LS. Cardiac steatosis in diabetes mellitus: a 1H-magnetic resonance spectroscopy study. *Circulation*. 2007;116:1170–1175. doi: 10.1161/CIRCULATIONAHA.106.645614
44. Muniyappa R, Noureldin R, Ouwerkerk R, Liu EY, Madan R, Abel BS, Mullins K, Walter MF, Skarulis MC, Gharib AM. Myocardial fat accumulation is independent of measures of insulin sensitivity. *J Clin Endocrinol Metab*. 2015;100:3060–3068. doi: 10.1210/jc.2015-1139

Supplemental Material

Data S1.

Imaging Acquisition Protocol by MDCT

MDCT scanning of the heart was performed by a 16-slice scanner (Sensation 16, Siemens Medical Solutions, Forchheim, Germany; 16×0.75 mm collimation, rotation time 420 ms and tube voltage 120 kV). In one breath-hold, images were acquired from above the level of the tracheal bifurcation to below the base of the heart using prospective ECG triggering with the center of the acquisition at 70% of the R-R interval. From the raw imaging dataset, images were reconstructed with standard kernel in 3-mm thick axial, non-overlapping slices and 25-cm field of view.

All axial images were loaded into a workstation (Aquarius 3D Workstation, TeraRecon, San Mateo, CA, USA). Multiplanar reconstructions of the MDCT data in standardized horizontal long-axis plane (Figure S1A) was used for IAF measurement (arrow, Figure S1A). To precisely define the plane used for IAF assessment, we adjusted the central lines across both left ventricular apex and the center of mitral annulus for the vertical long-axis plane (figure S1B); further adjustment of central lines across both the center of left atrium chamber and cardiophrenic angle at the basal level of left ventricle was used for the short-axis plane (Figure 1SC).

Diagnostic/Discriminative Performance of Region-specific Visceral Fat in Prevalent Diabetes

In the diabetes group, EAT, PAT, PARF, and TAT volumes were larger in obese than in lean participants (lean: obese 70.6±22.0 cm³ vs 89.8±27.3 cm³, 20.7±6.7mm vs 27.2±9.2mm, 18.7±8.8 cm³ vs 28.8±10.4 cm³, 6.7±3.0 cm³ vs 10.0±4.2 cm³, respectively, all $p<0.05$) but there was no difference in the IAF volume ($p=0.535$;

Figure 3). Each standardized increment of EAT, PAT, IAF, PARF, and TAT was associated with a higher baseline diabetes risk (adjusted OR: 1.5, 1.6, 2.0, 1.7, and 1.8) and higher probability of having either pre-prediabetes or known diabetes (adjusted OR: 1.2, 1.3, 1.5, 1.3, and 1.4), respectively (all $p < 0.01$). IAF and TAT superimposed on age, sex, BMI, and baseline HOMA-IR remarkably expanded the likelihood ratio of identifying baseline diabetes (χ^2 : from 67.2 to 86.0 and 64.4 to 70.8, p for $\Delta \chi^2$: < 0.001 and 0.011, respectively), which was not significant by adding EAT, PAT or PARF on the same baseline covariates (p for $\Delta \chi^2$: 0.65 and 0.48, respectively). The AUCs of EAT, PARF, IAF, and TAT were significantly greater than the AUC of body fat composition (AUC: 0.56) in identifying baseline diabetes (all $p < 0.05$). The AUCs of IAF, PARF and TAT were significantly larger than the AUC of BMI (AUC 0.62) in identifying baseline diabetes (all $p < 0.05$, Table 2).

Table S1. Univariable and multivariable-adjusted regressions for various visceral adiposity measures with dysglycemic indices and circulating pro-inflammatory markers.

	Univariate		Multivariate							
			Model 1		Model 2		Model 3		Model 4	
	<i>Beta</i> coef. (SE)	<i>p</i> value	<i>Beta</i> coef. (SE)	<i>p</i> value	<i>Beta</i> coef. (SE)	<i>p</i> value	<i>Beta</i> coef. (SE)	<i>p</i> value	<i>Beta</i> coef. (SE)	<i>p</i> value
Epicardial fat (EAT)										
Fasting glucose, mg/dL	0.134(0.028)	<0.001	0.152(0.086)	<0.001	0.034(0.033)	0.362	0.005(0.033)	0.892	0.007(0.032)	0.855
Postprandial glucose, mg/dL	0.082(0.066)	0.030	0.289(0.199)	<0.001	-0.015(0.073)	0.720	-0.047(0.072)	0.267	-0.030(0.070)	0.486
HbA1c, mg/dL	0.121(0.001)	0.001	0.208(0.003)	<0.001	-0.015(0.001)	0.705	-0.051(0.001)	0.196	-0.011(0.001)	0.787
HOMA-IR	0.202(0.002)	<0.001	-0.001(0.008)	0.978	0.083(0.003)	0.095	0.085(0.003)	0.008	0.119(0.003)	0.016
hs-CRP, mg/L	0.099(0.0002)	0.003	0.052(0.001)	0.117	0.034(0.033)	0.362	-0.024(0.0003)	0.537	-0.012(0.0004)	0.757
Neutrophil-to-lymphocyte ratio	0.059(1.004)	0.065	0.039(0.001)	0.248	0.016(0.001)	0.677	0.005(0.001)	0.897	0.003(0.001)	0.946
Paracardial fat (PAT)										
Fasting glucose, mg/dL	0.151(0.001)	<0.001	0.095(0.003)	0.001	0.049(0.001)	0.092	0.033(0.001)	0.255	0.064(0.001)	0.032
Postprandial glucose, mg/dL	0.113(0.001)	0.002	0.080(0.001)	0.029	0.605(0.001)	0.091	0.040(0.001)	0.268	0.040(0.001)	0.268
HbA1c, mg/dL	0.136(0.301)	<0.001	0.085(0.030)	0.010	0.025(0.031)	0.447	0.003(0.031)	0.937	0.038(0.031)	0.257
HOMA-IR	0.169(0.021)	<0.001	0.148(0.020)	<0.001	0.048(0.020)	0.254	0.048(0.020)	0.259	0.059(0.019)	0.152
hs-CRP, mg/L	0.091(0.110)	0.005	0.074(0.105)	0.018	-0.010(0.104)	0.741	-0.007(0.102)	0.813	0.003(0.103)	0.936
Neutrophil-to-lymphocyte ratio	0.113(0.029)	<0.001	0.103(0.035)	0.002	0.102(0.039)	0.005	0.096(0.039)	0.008	0.105(0.041)	0.005

Interatrial fat (IAF)

Fasting glucose, mg/dL	0.195 (0.920)	<0.001	0.137 (1.029)	<0.001	0.078 (1.073)	0.033	0.061 (1.079)	0.097	0.099 (1.030)	0.008
Postprandial glucose, mg/dL	0.242 (2.181)	<0.001	0.173 (2.440)	<0.001	0.132 (2.549)	0.002	0.112 (2.566)	0.009	0.161 (2.398)	<0.001
HbA1c, mg/dL	0.265 (0.036)	<0.001	0.212 (0.041)	<0.001	0.138 (0.041)	<0.001	0.118 (0.041)	0.003	0.156 (0.041)	<0.001
HOMA-IR	0.140 (0.084)	0.001	0.156 (0.303)	0.002	0.051 (0.098)	0.315	0.045 (0.099)	0.377	0.080 (0.099)	0.115
hs-CRP, mg/L	0.135 (0.009)	<0.001	0.137 (0.011)	<0.001	0.047 (0.013)	0.220	0.049 (0.011)	0.207	0.068 (0.012)	0.085
Neutrophil-to-lymphocyte ratio	0.118(0.030)	<0.001	0.102(0.038)	0.004	0.094(0.041)	0.013	0.088(0.041)	0.022	0.090(0.042)	0.021

Periaortic fat (PRAF)

Fasting glucose, mg/dL	0.207 (0.075)	<0.001	0.160 (0.079)	<0.001	0.122 (0.096)	0.002	0.085 (0.094)	0.030	0.087 (0.093)	0.035
Postprandial glucose, mg/dL	0.124 (0.176)	0.001	0.070 (0.183)	0.068	0.036 (0.217)	0.442	-0.007 (0.212)	0.876	0.012 (0.211)	0.801
HbA1c, mg/dL	0.200 (0.003)	<0.001	0.154 (0.003)	<0.001	0.080 (0.004)	0.068	0.036 (0.004)	0.391	0.083 (0.004)	0.063
HOMA-IR	0.250 (0.007)	<0.001	0.258 (0.007)	<0.001	0.118 (0.009)	0.031	0.130 (0.008)	0.014	0.168 (0.009)	0.002
hs-CRP, mg/L	0.149 (0.001)	<0.001	0.145 (0.001)	<0.001	-0.005 (0.001)	0.905	0.024 (0.001)	0.559	0.024 (0.001)	0.582
Neutrophil-to-lymphocyte ratio	0.098(0.361)	0.002	0.083(0.003)	0.013	0.102(0.039)	0.005	0.061(0.004)	0.135	0.051(0.004)	0.239

Thoracic aortic fat (TAT)

Fasting glucose, mg/dL	0.254 (0.215)	<0.001	0.221 (0.251)	<0.001	0.204 (0.285)	<0.001	0.174 (0.288)	<0.001	0.185 (0.272)	<0.001
Postprandial glucose, mg/dL	0.187 (0.519)	<0.001	0.147 (0.592)	0.001	0.147 (0.654)	0.002	0.114 (0.660)	0.018	0.139 (0.621)	0.004
HbA1c, mg/dL	0.255 (0.009)	<0.001	0.221 (0.010)	<0.001	0.189 (0.011)	<0.001	0.151 (0.011)	0.001	0.191 (0.011)	<0.001
HOMA-IR	0.246 (0.020)	<0.001	0.284 (0.024)	<0.001	0.143 (0.026)	0.010	0.139 (0.026)	0.013	0.178 (0.026)	0.001

hs-CRP, mg/L	0.203 (0.002)	<0.001	0.235 (0.003)	<0.001	0.134 (0.003)	0.002	0.148 (0.003)	0.001	0.165 (0.003)	<0.001
Neutrophil-to-lymphocyte ratio	0.137(0.128)	<0.001	0.142(0.009)	<0.001	0.150(0.011)	<0.001	0.140(0.011)	0.001	0.129(0.011)	0.003

Model 1: adjustment for age, sex;

Model 2: adjustment for age, sex, body mass index, total cholesterol, high density lipoprotein, estimated glomerular filtration rate;

Model 3: adjustment for age, sex, waist circumference, total cholesterol, high density lipoprotein, estimated glomerular filtration rate;

Model 4: adjustment for age, sex, body fat percentage, total cholesterol, high density lipoprotein, estimated glomerular filtration rate.

Beta coef.: *Beta* coefficient, SE: standard error.

BMI = body mass index; HbA1C = glycosylated hemoglobin; HOMA-IR = homeostasis model assessment of insulin resistance; hs-CRP = high sensitivity C-reactive protein.

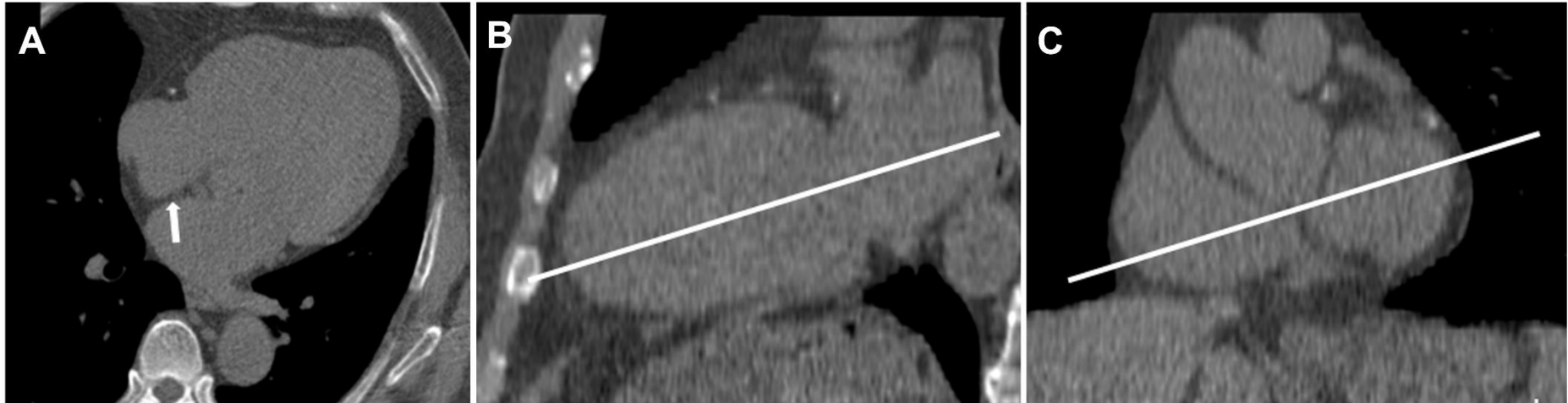
Table S2. Correlation coefficient (Pearson's r) between various visceral adiposity measures and anthropometric indices.

	Epicardial fat (EAT), cm³	Paracardial fat (PAT), mm	Interatrial fat (IAF), cm³	Periaortic fat (PARF), cm³	Thoracic aortic fat (TAT), cm³
Body mass index, kg/m²	0.470 (<i>p</i> <0.001)	0.383 (<i>p</i> <0.001)	0.434 (<i>p</i> <0.001)	0.587 (<i>p</i> <0.001)	0.484 (<i>p</i> <0.001)
Body fat composition, %	0.287 (<i>p</i> <0.001)	0.136 (<i>p</i> <0.001)	0.045 (<i>p</i> =0.163)	0.327 (<i>p</i> <0.001)	0.901 (<i>p</i> <0.001)
Waist circumference, cm	0.507 (<i>p</i> <0.001)	0.453 (<i>p</i> <0.001)	0.532 (<i>p</i> <0.001)	0.408 (<i>p</i> <0.001)	0.491 (<i>p</i> <0.001)

Table S3. Correlation coefficient (Pearson's r) between coronary calcium score and various visceral adiposity measures.

	Epicardial fat (EAT), cm³	Paracardial fat (PAT), mm	Interatrial fat (IAF), mm	Periaortic fat (PARF), cm³	Thoracic aortic fat (TAT), cm³
Coronary calcium score	0.28 (<i>p</i> <0.001)	0.08 (<i>p</i> =0.006)	0.15 (<i>p</i> <0.001)	0.23 (<i>p</i> <0.001)	0.20 (<i>p</i> <0.001)

Figure S1. Planes used for multiplanar reconstructions of the MDCT data for IAF measure



Standardized horizontal long-axis plane (A) for IAF assessment. Plane was adjusted by the central lines across left ventricular apex and the center of mitral annulus in the vertical long-axis plane (B) and across the center of left atrium chamber and cardiophrenic angle from ventricular short-axis plane at the basal level (C).